MODELLING ROUGH SURFACES WITH EDGE DIFFRACTION

UP Svensson Dept. of Telecommunications, Norwegian University of Science and Technology, Trondheim, Norway
RR Torres Program in Architectural Acoustics, Rensselaer Polytechnic Institute, Troy, New York, USA

1 INTRODUCTION

This paper studies the scattering from finite rough surfaces using specular reflection and edge diffraction impulse responses applied to polygonal deterministic approximations of such surfaces. This approach has been used earlier for the modelling of scattering from rough sea surfaces with the wedge assemblage (WA) method[1]. Here, we apply it to calculate the scattering coefficient, using the method by Mommertz[2], based on the reflected sound field in all directions over a half-space. Embrechts et al[3] studied the scattering coeffficient using the Kirchhoff approximation. They point out a number of well-known limitations for the Kirchhoff approximation which restricts its use in some ways. It is the purpose of this paper to compare calculations of the scattering coeffficient using both the Kirchhoff approximation and a method[4] which is derived from the exact Biot-Tolstoy edge diffraction impulse response expression[5]. This Biot-Tolstoy based method is valid for rigid surfaces only, which has been studied here. The wedge assemblage method is also based on the Biot-Tolstoy expression[1], and the difference between the WA method and the method used here lies in different, but equivalent, expressions for first-order diffraction, and different expressions for higher-order diffraction.

The Kirchhoff approximation has proven to be accurate in many cases[6]. The main limitations are that the incident and reflected sound waves must have angles that are smaller than approximately 60 degrees relative to the surface normal, and the correlation length of the plate's roughness profile must be greater than the wavelength. In underwater acoustics many situations seem to stay within these restrictions but in room acoustics where the sounds fields are more or less diffuse, the incidence and reflections angles will cover a wide range. Furthermore, the wall surfaces used in buildings rarely have the slowly undulating profile that the correlation length limitation implies.
A special type of surface used in rooms is the Schroeder-diffusor type. These have wells of different depths, quite sharp edges and do not directly fulfil the requirements for the Kirchhoff approximation. Cox has studied such surfaces extensively, using variants of 2D and 3D boundary element techniques[7]. The boundary element method can be considered a reference solution method which is efficient at low frequencies for full 3D modelling.

The scattering coefficient is an important input parameter for room acoustic prediction methods that use a stochastic approach to model surface scattering such as ray tracing or radiosity. The method used here is purely deterministic and can act as an important reference method for studying quite arbitrary geometries. On the other hand, it is not feasible to use such a deterministic method for modelling all rough surfaces of a large room. The most promising use of the specular reflection + edge diffraction methods in computational room acoustics is probably to correctly handle the influence of the finite sizes of larger wall elements, and scattering objects like railings and protruding edges. In addition in can serve as a alternative reference method for comparisons with simplified techniques. Being a time-domain method, it can also give insight into the statistical properties of the impulse responses of rough surfaces, which can be used for generating impulse responses that represent rough surfaces.

2 CALCULATION METHOD

2.1 Scattering coefficient

In this study the room acoustics scattering coefficient is the primary quantity that has been calculated. As shown by Mommertz[2], the scattering coefficient δ can be found from a detailed measurement, or prediction, of the scattered sound field from a finite rough surface, but also requires the response from a flat rigid reference surface. The scattering coefficient is then

$$\delta = 1 - \frac{\left| \sum_{i=1}^{n} p_1(\theta_i) p_0^*(\theta_i) \right|^2}{\sum_{i=1}^{n} \left| p_1(\theta_i) \right|^2 \sum_{i=1}^{n} \left| p_0(\theta_i) \right|^2} \qquad (1)$$

where p_1 is the (complex) amplitude of the reflected sound pressure from the scattering surface, and p_0 is the (complex) amplitude of the reflected sound pressure from the flat, rigid reference surface of the same size as the scattering surface. Both p_1 and p_0 should be measured/predicted in a number of directions θ_i. The expression in eq. (1) is based on the assumption that the scattered response is statistically independent from the flat reference surface response.

2.2 Diffraction modelling

As mentioned above, the approach used here, illustrated in Fig. 1, models scattering by finding the valid specular reflection and edge diffraction paths for a polygonal approximation of a rough surface. This method can be used both for the flat reference surface and the rough surface.

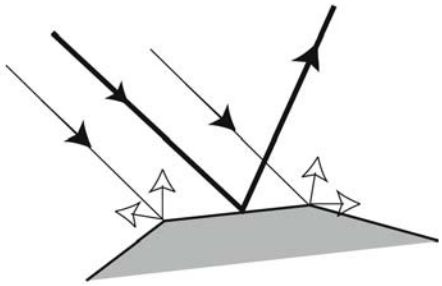

Figure 1 Illustration of a part of a rough surface which is modelled as a polygonal approximation. A specular reflection is shown in heavy line and edge diffraction waves are indicated by thinner lines.

Different methods are available for edge diffraction modelling[4,8,9]. For rigid or pressure-release surfaces exact expressions exist for the impulse responses of infinite wedges[4,5] and they are the basis for the method used here[4]. Specular reflections are taken into account with the ordinary image source method (employing visibility and obstruction checks), and the edge diffraction components are included using similar visibility and obstruction checks[10]. The edge diffraction impulse responses are calculated by placing secondary sources along each edge. The contribution from an edge to the total impulse response, $h_p(t)$, is then described by a line integral along the edge coordinate z,

$$h_p(t) = -\frac{\nu}{4\pi} \int_{z_1}^{z_2} \delta\left(t - \frac{m+l}{c}\right) \frac{\beta}{ml} dz, \qquad (2)$$

where β is a directivity function for the secondary edge sources. These impulse responses will be denoted ED-IRs in the following, for Edge Diffraction Impulse Responses. Depending on which

directivity function is chosen, different models can be implemented. The new method[4], is implemented using the following source directivities,

$$\beta_{new} = \beta_{++} + \beta_{+-} + \beta_{-+} + \beta_{--}, \tag{3a}$$

$$\text{where } \beta_{\pm\mp} = \frac{\sin\left[\nu\left(\pi \pm \theta_S \mp \theta_R\right)\right]}{\cosh \nu\eta - \cos\left[\nu\left(\pi \pm \theta_S \mp \theta_R\right)\right]} \tag{3b}$$

$$\text{and } \eta = \cosh^{-1}\frac{1+\sin\alpha\cdot\sin\gamma}{\cos\alpha\cdot\cos\gamma}. \tag{3c}$$

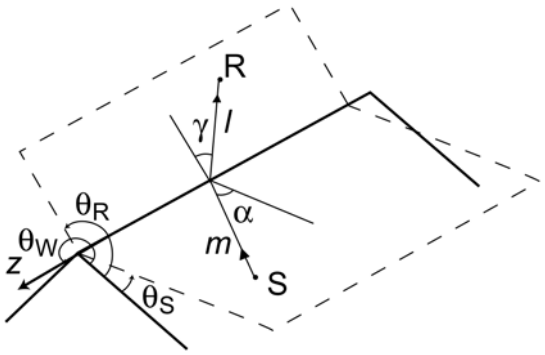

Figure 2 The geometry of an edge that is created by two semi-infinite planes drawn with solid lines, with a source position, S, and a receiver position, R, indicated. The planes drawn with dashed lines are virtual planes that contain S and R.

As illustrated in Fig. 2, the angles θ_S and α are the incidence angles for the wave hitting an edge position *z*, and the angles θ_R and γ are the scattering angles towards the receiver. The wedge angle is described by θ_w, $\nu = \pi / \theta_w$ is the wedge index, and *m* and *l* are the path lengths to and from the edge point. The Kirchhoff approximation is also possible to write in this form, by rewriting the line integral expression that result from the Maggi-Rubinowicz transformation[8]:

$$\beta_{Kirchhoff} = a_1\beta_1 + a_2\beta_2 \tag{4a}$$

$$\text{where } \beta_1 = \frac{\sin\left(\theta_S + \theta_R\right)}{\cosh\eta + \cos\left(\theta_S + \theta_R\right)} + \frac{\sin\left(\theta_S - \theta_R\right)}{\cosh\eta + \cos\left(\theta_S - \theta_R\right)}, \tag{4b}$$

$$\beta_2 = \frac{\sin\left(2\theta_W - \theta_S - \theta_R\right)}{\cosh\eta + \cos\left(2\theta_W - \theta_S - \theta_R\right)} + \frac{\sin\left(\theta_R - \theta_S\right)}{\cosh\eta + \cos\left(\theta_R - \theta_S\right)} \tag{4c}$$

$$\text{and } a_i = \begin{cases} 0 & \text{if plane } i \text{ can not be seen from both S and R} \\ 1 & \text{if plane } i \text{ can be seen from both S and R} \end{cases} \tag{4d}$$

It should be noted that the term $\cosh\eta$ in eqs. (4b) and (4c) leads to a cancelling of the cosh function, see the definition of η in eq. (3c). This implementation of the Kirchhoff approximation also gives edge diffraction impulse responses, ED-IRs, so it is straightforward to run a direct comparison between the two methods.

When impulse responses are calculated, the sampling frequency must be high enough to give low enough temporal errors, which translates to accurate phase response when the impulse responses are transformed to transfer functions. For cases where there are both specular reflections and edge diffraction components that arrive close in time, very accurate temporal responses are needed. Here the specular reflections are generated by letting a continuous-time dirac pulse be represented by two pulses in the two time samples nearest the exact arrival time, and a simple linear weighting as used by Vanderkooy[11]. This scheme leads to an accurate phase response of the corresponding

transfer function but a magnitude roll-off at relatively low frequencies. The ED-IRs are calculated with the approach in Ref. 4, which for most source-receiver geometries can employ a simplified numerical integration. For using eq. (1), the impulse responses are transformed to the frequency domain.

2.3 Surface generation

A rough plate was simulated by giving a rectangular plate a random profile. To keep the computational load down, a one-dimensional random profile was chosen even if the method can handle plates with two-dimensional random profiles[1] and even arbitrary three-dimensional objects as long as they are approximated as polygonal assemblages. A square rigid plate, 1 m by 1 m, was divided into 255 parallel strips that were generated by dividing one of the two plate edges into 256 evenly distributed points. These points were then given a random height (perpendicular to the plate) according to a gaussian distribution. A desired correlation length was implemented by convolving this random sequence with the corresponding "smearing filter", equivalent to the method used by Thorsos[6] and Embrechts et al[3]. A simple gaussian profile was chosen in order to make comparisons with other results easier even though arbitrary distributions could be defined.

3 RESULTS

3.1 Calculation parameters

Samples of rough, perfectly rigid, 1m by 1m plates were generated with four different correlation lengths, as described in section 2.3. Fig. 3 shows the profiles of these plates, with the correlation lengths 512 mm, 256 mm, 128 mm and 64 mm. In addition, a flat rigid plate was used for the reference case which is needed for calculating the scattering coefficient according to eq. (1).

Figure 3 Profiles of plate realizations with different correlation lengths. The plates have a side length of 1 m and a roughness with a standard deviation σ = 18 mm. The correlation lengths are, from left to right, 512 mm, 256 mm, 128 mm, and 64 mm.

A single source was placed in the far field, at a distance of 1000 m, either right above the plate, i.e., with an incidence angle of 0 degrees, or with an incidence angle of 45 degrees. Receiver positions were distributed at the same distance over the hemisphere above the plate. A total of 638 receiver positions were used so that the maximum angle difference (in the θ- and φ-directions) between adjacent receiver positions was 6 degrees. A weighting factor is introduced into eq. (1) to take into account that the 638 receiver positions represent slightly different solid angles. For the chosen plate size, the used angular resolution should be sufficient for frequencies up to 2.8 kHz according to the criterion suggested by Embrechts et al[3]. For all plates, the same roughness amplitude was used, with a standard deviation, σ, of 18 mm.

Edge diffraction impulse responses, ED-IRs, were calculated for each of the plates and for all receiver points. Both the new method, eqs. (2)-(3), and the Kirchhoff impulse response method, eqs. (2),(4) were used for all cases. In the results diagrams, these results will be marked as "New ED-IR" and "Kirchhoff ED-IR", respectively. Also, the results using the "characteristic function" model, presented by Embrechts et al[3] are included here. It should be noted that this function is based on the Kirchhoff approximation and gives the scattering coefficient as

$$\delta = 1 - \left| \frac{1}{n} \sum_{i=1}^{n} \exp\left(-2jk\xi_i \cos\theta_{in}\right) \right|^2 \qquad (5)$$

where ξ_i are the profile heights along the plate. This characteristic function is expected to give results that are similar to the Kirchhoff ED-IR method, as long as the assumptions behind the Kirchhoff approximation are fulfilled.

3.2 Influence of correlation length

As pointed out by Embrechts et al[3], the Kirchhoff modelling requires that the relations between the plate size, L_x, the correlation length, T, the surface roughness, σ, and the wavelength, λ, fulfill $T > \lambda$, $T > 2\sigma$, $T << L_x$. This was studied for the four different plates in Fig. 3. All of these four plates fulfil $T > 2\sigma$. The length of the plate, L_x, is clearly not much larger than T for the first plates. The first criterion that is listed, $T > \lambda$, will give different frequency ranges for the four plates.

Examples of ED-IRs for the reference plate and the two plates with correlation lengths of 512 mm and 256 mm are shown in Fig. 4 together with the corresponding transfer functions. The sound incidence was perpendicular, and a receiver position was placed at 42 degrees relative to the surface normal, and with an azimuthal angle of 42 degrees. All three responses have roughly the same length in time, with a similar positive first half and negative second half. The varying heights of the rough plates clearly distort the basic shape of the flat plate, and the sharper the peaks of the plate profile, the sharper peaks will be seen in the plate impulse response. If higher-order diffraction components are included, they will show up as weaker components spread out over longer time. For plates with steeper slopes and for more grazing source/receiver angles there will also be specular-diffraction combinations. In the frequency domain, the three responses are very similar at low frequencies, as expected, and with interference patterns that are also quite similar at low frequencies.

One interesting observation that could be used for generating stochastic impulse responses that should represent rough surfaces is that for plates with large numbers of peaks and valleys in the profile, there will be quite a noise-like response within the time-window defined by the plate size. Such a noise-like response, with the correct level and spectral shape, could then be used for generating stochastic impulse responses.

The scattering coefficient was calculated using eq. (1) and the results are shown in Fig. 5, for the perpendicular sound incidence. Results calculated with both the new ED-IRs and the Kirchhoff ED-IRs are presented, together with the characteristic function result in Eq. (5).

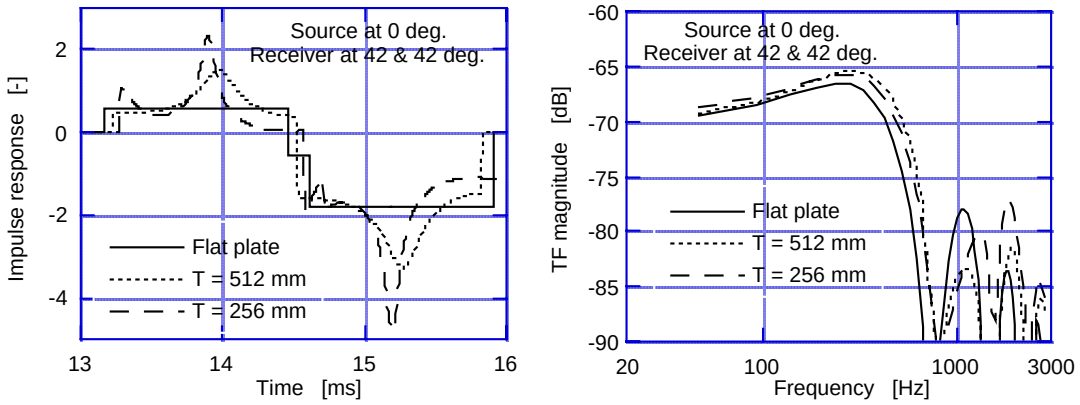

Figure 4 Examples of edge diffraction impulse responses and the corresponding transfer functions for the flat plate and the two plates with the longest correlation lengths in Fig. 4. The sound incidence was perpendicular and the receiver was placed at 42 degrees relative to the

surface normal and with an azimuthal angle of 42 degrees. The time scale and the impulse response scale use arbitrary references. The transfer function is relative to the incident sound wave. A few things can be observed in Fig. 5: first, the new method and the Kirchhoff method generally agree very well but differ at lower frequencies. The frequency range that should be valid for the Kirchhoff approximation according to the criterion $T > \lambda$ is indicated with the grey bar on the horizontal axis and it can be seen that the Kirchhoff ED-IR results and the results with the new ED-IR method deviate more outside this range. A bit surprisingly, the characteristic function results agree well with the new ED-IR results, even when the Kirchhoff ED-IR results differ.
Finally, it can also be seen that for the lowest frequencies, which corresponds to the lowest values of σ/λ, the calculated values of the scattering coefficient seem too high, with both the new ED-IR method and the Kirchhoff ED-IR method. This indicates that there could be a need to include multiple diffractions, and this is especially pronounced for the shortest correlation length. It should be noted that the scale for σ/λ is linear, as opposed to the logarithmic frequency scale in Fig. 4, in order to focus on the frequency range where the scattering coeffficient is changing the most.

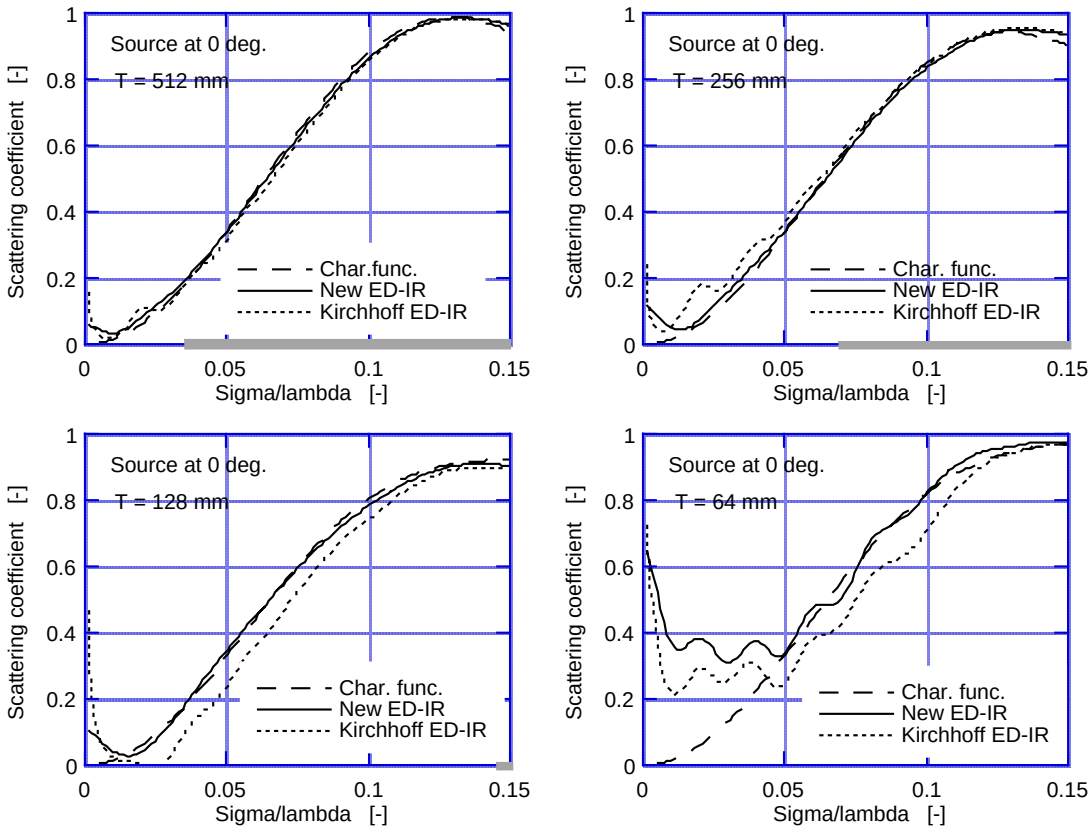

Figure 5 Scattering coefficient for the four plates in Fig. 3 with the correlation lengths (a) 512 mm, (b) 256 mm, (c) 128 mm, and (d) 64 mm. The roughness had a standard deviation of 18 mm and the sound incidence was perpendicular. The grey bars on the σ/λ-axis indicate the validity region for the Kirchhoff approximation ($T>\lambda$).

3.3 Non-perpendicular incidence

A second source position was run, with an angle of incidence of 45 degrees, which should be within the validity region for the Kirchhoff approximation. Fig. 6 shows the calculated scattering coefficients for this source position and it can be seen that in general, the deviation between the new ED-IR method and the Kirchhoff ED-IR method is larger for lower frequencies, and for shorter correlation lengths, in the same way as for the perpendicular incidence of Fig. 5. Quite large deviations result for the correlation length of 128 mm but this case is outside the valid frequency range for the Kirchhoff approximation. It could be argued that the new method gives more accurate results since

it doesn't suffer from the inherent limitations of the Kirchhoff approximation. On the other hand there are no clear rules for determining how many orders of diffraction that should be included and since this strongly affects the computation time, more tests are needed.

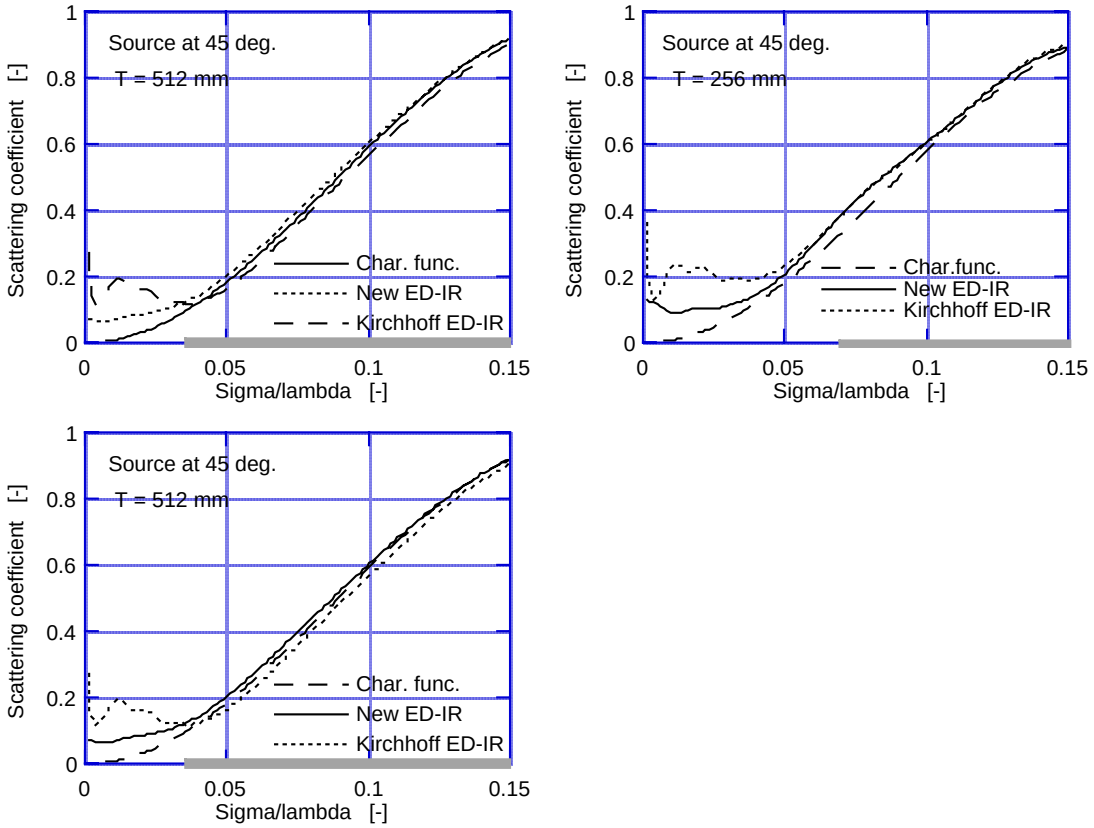

Figure 6 Scattering coefficient for three of the four plates in Fig. 3. Legends are the same as in Fig. 5.

4 CONCLUSIONS

Two methods have been demonstrated for the deterministic modelling of a rough rigid surface, both based on edge diffraction impulse responses. One is an implementation of the Kirchhoff approximation and the other is based on a new method which is exact for infinite wedges. Single realizations of rough surfaces were studied with the two methods and they seem to agree well as long as the correlation length T is larger than the wavelength λ, and this agrees with established criteria for the Kirchhoff method. However, for realistic surface models quite much shorter correlation lengths would be needed. The new method could handle such cases but would also require an effficient and accurate handling of all specular-diffraction combinations.

The calculated scattering coefficients for single realizations are also very close to the expected results based on the so-called characteristic function, which is based on the Kirchhoff approximation. This supports the possibility to use the simple theoretical expressions for slowly varying surfaces.

Further research is needed for comparing these results with reference solutions. The need for multiple orders of diffraction will be addressed in future studies. Also, edge diffraction solutions for non-rigid surfaces need to be developed. in order to study more realistic surfaces.

5 ACKNOWLEDGEMENTS

The first author's research was funded by the Research Council of Norway, in the Acoustic Research Centre project.

6 REFERENCES

1. R. S. Keiffer and J. C. Novarini, 'A time domain rough surface scattering model based on wedge diffraction: Application to low-frequency backscattering from two-dimensional sea surfaces', J. Acoust. Soc. Am. 107 27-39 (2000).
2. E. Mommertz, 'Determination of scattering coefficients from the reflection directivity of architectural surfaces', Appl. Acoust. 60 201-203 (2000).
3. J. J. Embrechts, D. Archambeau, and G. B. Stan, 'Determination of the scattering coefficient of random rough diffusing surfaces for room acoustics applications', Acta Acustica/Acustica 87 482-494 (2001).
4. U. P. Svensson, R. I. Fred, and J. Vanderkooy, 'Analytic secondary source model of edge diffraction impulse responses', J. Acoust. Soc. Am. 106 2331-2344 (1999).
5. M. A. Biot and I. Tolstoy, 'Formulation of wave propagation in infinite media by normal coordinates with an application to diffraction', J. Acoust. Soc. Am. 29 381–391 (1957).
6. E. I. Thorsos, 'The validity of the Kirchhoff approximation for rough surface scattering using a gaussian roughness spectrum', J. Acoust. Soc. Am. 83 78-92 (1988).
7. T. J. Cox, 'Predicting the scattering from reflectors and diffusers using two-dimensional boundary element methods', J. Acoust. Soc. Am. 96 874-878 (1994).
8. Y. Sakurai and K. Nagata, 'Sound reflections of a rigid plane and of the "live end" composed by those panels', J. Acoust. Soc. Jpn 2 5-14 (1981).
9. H. Medwin, E. Childs and G. M. Jebsen, 'Impulse studies of double diffraction: A discrete Huygens interpretation', J. Acoust. Soc. Am. 72 1005–1013 (1982).
10. R. R. Torres, U. P. Svensson and M. Kleiner, 'Computation of edge diffraction for more accurate room acoustics auralization', J. Acoust. Soc. Am. 109 600-610 (2001).
11. J. Vanderkooy, 'A simple theory of cabinet edge diffraction', J. Aud. Eng. Soc. 39 923–933 (1991).